Weak lasing in one-dimensional polariton superlattices

Long Zhang[a,1], Wei Xie[a,1], Jian Wang[a], Alexander Poddubny[b], Jian Lu[a], Yinglei Wang[a], Jie Gu[a], Wenhui Liu[a], Dan Xu[a], Xuechu Shen[a], Yuri Rubo[c], Boris Altshuler[d], Alexey Kavokin[e] and Zhanghai Chen[a,2]

[a]*State Key Laboratory of Surface Physics, Key Laboratory of Micro and Nano Photonic Structure (Ministry of Education), Department of Physics, Fudan University, Shanghai 200433, China*

[b]*Ioffe Physical-Technical Institute of the Russian Academy of Sciences, St-Petersburg 194021, Russia*

[c]*Instituto de Energías Renovables, Universidad Nacional Autónoma de México, Temixco, Morelos 62580, Mexico*

[d]*Physics Department, Columbia University, New York, New York 10027, USA*

[e]*Spin Optics Laboratory, St-Petersburg State University, 1, Ulianovskaya, St-Petersburg, Russia and Physics and Astronomy School, University of Southampton, Highfield, Southampton, SO171BJ, UK*

[1] L. Z. and W. X. contributed equally to this work.

[2]To whom correspondence should be addressed. e-mail: zhanghai@fudan.edu.cn

Classification: physical sciences, physics

Corresponding author: name: Zhanghai Chen

address: Han Dan Road NO.220, Shanghai, China

telephone number: +8602151630251

e-mail address: zhanghai@fudan.edu.cn

Keywords: polariton | condensates | weak-lasing | superlattice

Author contributions：The experiments were carried out by L.Z., W.X., J.W., J.L., W.L., D.X., Y.W., J.G., X.S., and Z.C. They have been interpreted by Z.C., Y.R., B.A. and A.K. The life-time calculations were done by A.P. and L.Z. The paper has been written by Z.C., Y.R., B.A., A.K., L. Z., W. X. and A.P. All authors discussed the results.

Abstract:

Bosons with finite life-time exhibit condensation and lasing when their influx exceeds the lasing threshold determined by the dissipative losses. In general, different one-particle states decay differently, and the bosons are usually assumed to condense in the state with the longest life-time. Interaction between the bosons partially neglected by such an assumption can smear the lasing threshold into a threshold domain – a stable lasing many-body state exists within certain intervals of the bosonic influxes. This recently described *weak lasing*[1] regime is formed by the spontaneously symmetry breaking and phase-locking self-organization of bosonic modes, which results in an essentially many-body state with a stable balance between gains and losses. Here we report the first observation of the weak lasing phase in a one-dimensional condensate of exciton-polaritons[2,3] subject to a periodic potential. Real and reciprocal space photoluminescence images demonstrate that the spatial period of the condensate is twice as large as the period of the underlying periodic potential. These experiments are realized at room temperature in a ZnO microwire deposited on a silicon grating. The period doubling takes place at a critical pumping power, while at a lower power polariton emission images have the same periodicity as the grating.

Significance:

Bose-Einstein condensation of polaritons in periodically modulated cavities is a very interesting fundamental effect of the physics of many-body systems. It is also promising for application in solid-state lighting and information communication technologies. By a simple micro-assembling method, we created periodically modulated polariton condensates at room temperature, and observed the stabilization of the coherent condensate due to the spontaneous symmetry breaking transition. This manifests a new type of phase transition, leading to a novel state of matter: the weak lasing state. The optical imaging in both direct and reciprocal space provides a clear evidence for the weak lasing in the specific range of the pumping intensities.

The application of artificial periodic potentials to electrons and photons causes a rich variety of phenomena, from electronic minibands in semiconductor superlattices to characteristic stop bands in photonic crystals[4-7]. These phenomena form the basis for further developments of opto-electronics. Cavity polaritons (quasi-particles formed by the strong coupling of confined photons with excitons) attracted much attention in recent years due to the remarkable coherent effects linked to their half-matter half-light nature[8-12]. As a result, a new area of physics at the boundary between solid-state physics and photonics has emerged.

Experiments on spatially-inhomogeneous polariton condensation are usually interpreted assuming that all one-particle states have the same life-time[13,14]. Lifting-off this assumption led to the prediction[1] of the "weak lasing" state of interacting polaritons: a new type of condensate stabilized by the spontaneous reduction of the symmetry rather than by the dissipation nonlinearities due to, e.g., reservoir depletion. In this work we report the first experimental

observation of room-temperature polariton condensation in one-dimensional (1D) superlattices, which brings clear evidence for the weak lasing state.

The polariton superlattice was assembled using a ZnO microrod with a hexagonal cross section: a natural whispering gallery resonator to efficiently confine exciton-polaritons[15,16]. Setting the microrod on a silicon slice with periodically arranged channels (**Figure 1**) allowed us to avoid the intrinsic structural diffraction typical for the structures with periodic patterns deposited on top of microcavities[17].

The polaritons in this structure were created by non-resonant continuous wave (or long pulse) optical pumping at room temperature and they were characterized by angle-resolved and spatially resolved photoluminescence (ARPL and SRPL) from the top of the microcavity. The periodic potential caused by the silicon grating manifested itself by a characteristic folded dispersion of the lower polariton branch, revealed in the ARPL images (**Figure 2**). One can see the avoided crossing of the polariton dispersion branches resulting in a distinct band gap near the Bragg plane. At strong enough pumping the polariton condensation demonstrates a striking feature: the condensate is formed at the *excited polariton states* near the energy gaps (states A, **Figure 3a**) rather than at the ground state: the π-state condensate[17].

We checked the spatial coherence of condensates at state A by interferometry experiments. **Figure 3(e,f)** shows two SRPL images of the condensates coming from the two arms of the Michelson interferometer; **Figure 3f** shows the inversion of the pattern **Figure 3e** by a retro-reflector. **Figure 3g** shows the interference pattern created by the superposition of the two images with the relative time delay smaller than the coherence time of the polariton condensate (~3 picoseconds). The arrows indicate unambiguous interference fringes between two condensates separated by 6 micrometers. The interference patterns can be observed even for a separation as large as 10 micrometers, i.e., the π-state condensate[17] in our superlattices indeed demonstrates a long-range coherence.

Besides creating the potential wells for polaritons, the contacts of the ZnO microrod with the patterned Si substrate affect the polariton dissipation: in the contact regions (inside the wells) the losses are stronger. This effect naturally explains the π-state condensation: as it is shown in **Figure 3c** the minima of the probability amplitude of the state A are at the contact regions, i.e., the polaritons in this state live longer than in the other state A′ at the edge of the Brillouin zone, which has maxima at the contact regions. The ground state D with zero wave vector k is distributed between the wells and the barriers more equally and thus possesses an intermediate life-time. The presence of long-living states at the Bragg gap edges has been previously observed in experiments on X-ray diffraction in crystals[18] and referred to as the Borrmann effect. A similar effect is known to suppress light localization in disordered photonic crystals[19]. We calculated the lifetime of polariton states for the different folded dispersion branches in the simplified Kronig-Penney model (See the Supplementary Information for details) and found that in the A-state the polaritons indeed live longer than in the states A' and D, as shown in **Figure 3b** (red color corresponds to the longer lifetime): $\tau_A > \tau_D > \tau_{A'}$.

It is safe to assume that all polariton states within the Brillouin zone have approximately the same influx rate W, which is proportional to the external pumping rate P. Accordingly, as W

increases, the lasing condition $W\tau \geq 1$ is satisfied for the A state first. Given the period of the structure a, the emission from this state contains plane waves with wave vectors $k_{\|} = \pm\pi(2n + 1)/a$, where $n = 0, \pm1, \pm2, \ldots$.

However, the condensate in the A state becomes unstable for interacting polaritons at the second threshold $W_2 > W_1 = \tau_A^{-1}$ (see supporting information for details). The condensed state for $W > W_2$ is stabilized by the gradually increasing admixture of the D state to the A state. The experimental values of pumping that correspond to the first and the second threshold are $P_1 \approx 10$ nW and $P_2 \approx 20$ nW. The admixture of the D state is the manifestation of the weak-lasing regime[1] characterized by a spontaneous symmetry breaking. Indeed, the condensate wave function can be written as

$$\Psi(z) = C_A\psi_A(z) + C_D\psi_D(z), \quad (1)$$

where $\psi_{A,D}$ are the single-polariton wave functions of the A and D states, and the polariton density $|\Psi(z)|^2$ in this state is not periodic with the period a of the underlying lattice. Instead, it is periodic with the period $2a$. As we show in supporting information, the weak lasing condensate can be formed in two equivalent states, with coefficients $C_{A,D}$ having the same signs in one state and opposite signs in the other. Since the signs of $\psi_A(z)$ are opposite in the neighboring barriers, the amplitude $|\Psi(z)|$ in the odd barriers is larger than in the even ones. In contrast, the signs of $\psi_D(z)$ are the same at neighboring barriers, such that the amplitude $|\Psi(z)|$ in the odd barriers is smaller than in the even ones. In both cases, the condensate acquires the *double period* $2a$, and in addition to the pure A-state emission pattern there appears an emission line at $k_{\|} = 0$ (with possible weak satellites at $k_{\|} = \pm 2\pi n/a$).

We observed the period doubling of the polariton condensate in both ARPL and SRPL images (**Figure 4)**. At low pumping, the emission has the same periodicity in real space as the superlattice, while for pumping above the second threshold of about 20 nW the emission pattern doubles its period. We have checked that for $P > 20$ nW the three peaks at $k_{\|} = 0, \pm\pi/a$ in **Figure 4c** indeed correspond to the same frequency and are mutually coherent. At large pumping, the ratio of the intensity of the $k_{\|} = 0$ peak to the intensity of the $k_{\|} = \pm\pi/a$ peaks saturates at about 0.6, which is substantially smaller than the theoretically expected saturation value 1.5 for an ideal 1D lattice. This discrepancy is presumably due to the strong disorder present in the ZnO microrod, which is clearly seen from fluctuations in the amplitudes of the peaks in **Figure 4d**.

Previous low-temperature experiments on GaAs-based polariton superlattices[17] evidenced polariton lasing from the edge of the Brillouin zone but no period doubling. We believe that the weak-lasing phase in ZnO polariton superlattices is robust because both real and imaginary parts of the periodic potential are modulated much stronger than in the planar GaAs microcavity with a metallic pattern on the top studied in Ref. 17.

In conclusion, by the non-resonant optical pumping of a ZnO microrod / Si grid superlattices we created a condensate of exciton-polaritons at room temperature and proved its long-range phase coherence. At sufficiently strong pumping the spatial period of the condensate turned out to be twice as long as the period of the superlattice. This spontaneous symmetry breaking

strongly suggests that the weak-lasing regime of polariton condensation has been achieved in our experiments.

Materials and Methods

The experimental setup is detailed in Ref. 16. The ZnO microwires used here were synthesized by a chemical vapor deposition method. Instead of directly depositing a periodic pattern on the top surface of a microcavity, which might induce intrinsic structural diffraction, we laid the ZnO microrod on a silicon slice with periodically arranged channels. They contacted closely due to the Van der Waals force. This micro-assembled structure introduced an additional modulation to the ZnO polariton energies and lifetimes in the **z**-direction (crystallographic **c**-direction). The resonance energies of the cavity are shifted due to the variation of the effective refractive index induced by the silicon substrate, which results in the appearance of a superlattice potential. In order to characterize the polariton states in this structure we detected the photoluminescence signal from the top surface of the microcavity.

Acknowledgements

We thank Jacqueline Bloch, Eugenius Ivchenko, and Igor Aleiner for many stimulating discussions. The work is funded by the 973 projects of China (No. 2011CB925600), NSFC (No. 91121007, No. 11225419, No. 11304042), and the EU FP7 IRSES Project POLAPHEN. AP acknowledges the support of the "Dynasty" foundation and Russian President Grant No. MK-6029.2014.2. A.K. acknowledges the support from the Russian Ministry of Education and Science (contract N 11.G34.31.0067).

References:

1. Aleiner IL, Altshuler BL, Rubo YG (2012) Radiative coupling and weak lasing of exciton-polariton condensates. *Phys. Rev. B* 85, 121301.
2. Hopfield JJ (1958) Theory of the contribution of excitons to the complex dielectric constant of crystals. *Phys. Rev. Lett.* 112, 1555.
3. Deng H, Weihs G, Santori C, Bloch J, Yamamoto Y (2002) Condensation of semiconductor microcavity exciton polaritons. *Science* 298, 199-202.
4. Esaki L, Chang LL (1974) New transport phenomenon in a semiconductor "superlattice". *Phys. Rev. Lett.* 33, 495.
5. Robertson M, Arjavalingam G (1992) Measurement of photonic band structure in a two-dimensional periodic dielectric array. *Phys. Rev. Lett.* 68, 2023.
6. Colvard C, Merlin R, Klein MV, Gossard AC (1980) Observation of Folded Acoustic Phonons in a Semiconductor Superlattice. *Phys. Rev. Lett.* 45, 298–301.
7. Brückner R, et al. (2012) Phase-locked coherent modes in a patterned metal-organic microcavity. *Nature Photon.* 6, 322-326.

8. Weisbuch, C (1992) Observation of the coupled exciton-photon mode splitting in a semiconductor quantum microcavity. *Phys. Rev. Lett.* 69, 3314.
9. Amo A, et al. (2009) Collective fluid dynamics of a polariton condensate in a semiconductor microcavity. *Nature* 457, 291-296.
10. Wertz E, et al. (2010) Spontaneous formation and optical manipulation of extended polariton condensates. *Nature Physics*, 6, 860.
11. Sich M, et al. (2012) Observation of bright polariton solitons in a semiconductor microcavity. *Nature Photon.* 6, 50-55.
12. Sanvitto D, et al. (2010) Persistent currents and quantized vortices in a polariton superfluid. *Nature Phys*. 6, 527-533.
13. Wouters M, Carusotto I (2007) Excitations in a Nonequilibrium Bose-Einstein Condensate of Exciton Polaritons. *Phys. Rev. Lett*. 99, 140402.
14. Carusotto I, Ciuti, C (2013) Quantum Fluids of Light. *Rev. Mod. Phys*. 85, 299.
15. Sun LX et al. (2008) Direct observation of whispering gallery mode polaritons and their dispersion in a ZnO tapered microcavity. *Phys. Rev. Lett.* 100, 156403.
16. Xie W, et al. (2012) Room-temperature polariton parametric scattering driven by a one-dimensional polariton condensate. *Phys. Rev. Lett.* 108, 166401.
17. Lai CW, et al. (2007) Coherent zero-state and π-state in an exciton-polariton condensate array. *Nature* 450, 529-533.
18. Borrmann G (1950) Die Absorption von Röntgenstrahlen im Fall der Interferenz. *Zeitschrift für Physik* 127, 297.

Figure legends:

Figure 1 | Illustration of the assembled polaritonic superlattice based on a ZnO-Si microstructure. a, Schematic representation of the 1D polaritonic crystal. **b**, Scanning electron microscope image (top-view) of a ZnO microrod with hexagonal cross section placed on a periodic Si grating. The 1 μm-wide silicon channels equally spaced with the internal distance a= 2 μm apply a static periodic potential to the polaritons with amplitude $ReU \approx 2$ meV. The "s" and "f" mark the silicon-contacting parts and the free standing parts of the microcavity respectively. **c,d**, Angle-resolved photoluminescence (ARPL) spectral images taken under continuous He-Cd laser (325 nm) excitation. TE (electric field component of light along the z-axis) polariton modes are shown. **c**, Emission from a free standing ZnO microrod. The white dashed curves are theoretical fits of the lower polartion branches. **d**, The same ZnO microwire lying on a flat silicon surface. The peak position and the lineshape at $k_{||}$=0 are identified. The horizontal dashed lines indicate the LP energy shift (ReU). The incidence angle ϕ is linked with the in-plane wave vector of light by $k_{||} = (E/\hbar c)\sin\phi$, where E is the photon energy.

Figure 2 | Dispersion of exciton-polaritons in momentum space demonstrating formation of a polariton superlattice. a, PL mapping (second derivative) in $\boldsymbol{k}$-space under continuous excitation at room temperature. White dashed curves display the calculated dispersion with a band gap (ΔE = 0.7 meV). **b**,**c**, Enlarged regions identified by the dashed rectangles in **a** respectively, exhibiting the anti-crossing dispersion and well-resolved energy gap.

Figure 3 | Polariton condensation at the π-states. a. Polariton lasing at the edges of the mini-Brillouin zone in ***k***-space at room temperature. White dashed curves display the calculated dispersion with a band gap ΔE = 0.7 meV. **b**, Wavevector and energy dependence of the exciton-polariton radiative lifetime (calculated). The color scale is in units of picoseconds (red color represents longer lifetime). **c,** Real and imaginary parts of the complex potential induced by the Si grating for the microrod polaritons. The "air" and "silicon" represent the free standing parts and silicon-contacting parts of the microcavity. The bottom panel is the sketch of the probability amplitude distribution ($|\Psi|^2$) for the states labeled as A and A′ in Fig. 3b. **d**, Spatially resolved PL image obtained by exciting the microrod step-by-step along the **z** axis. The full width at half maximum of the pulsed excitation laser is about 1 μm. The emission bright regions are pinned to the period potential. **e-g**, Spatial coherence analysis from a Michelson interferometer. **e,f,** Real-space PL mappings measured by each arm of the interferometer. **f,** The second arm with a retro-reflector flips the image **e**. The excitation source in this experiment was a pulsed laser (wavelength: 355 nm, diameter of the laser spot: 10 μm). The top sketch shows the corresponding structure of the substrate. **g,** The coherent overlapping between the two images of the condensates forms the interference pattern. The interference fringes appear because of a small inclination angle between the images from the two arms of the interferometer.

Figure 4 | Phase transition from π-state condensation to weak lasing. **a**, The evolution of polariton condensates in momentum space with increasing pump power. The experiments were carried out on another sample. **b**, The power dependence of the PL intensity at the lasing frequency in ***k***-space. At the threshold of about 20 nW, a small peak appears at $k_{//}$=0. Its frequency corresponds to the edges of the Brillouin zone. **c**, The evolution of the polariton condensate's distribution in real space with increasing excitation power. **d**, The power dependence of the PL intensity at the lasing frequency in real space. At the threshold of 20 nW，the period of the polariton condensate is doubled compared to the period of the superlattice.

Figure 1

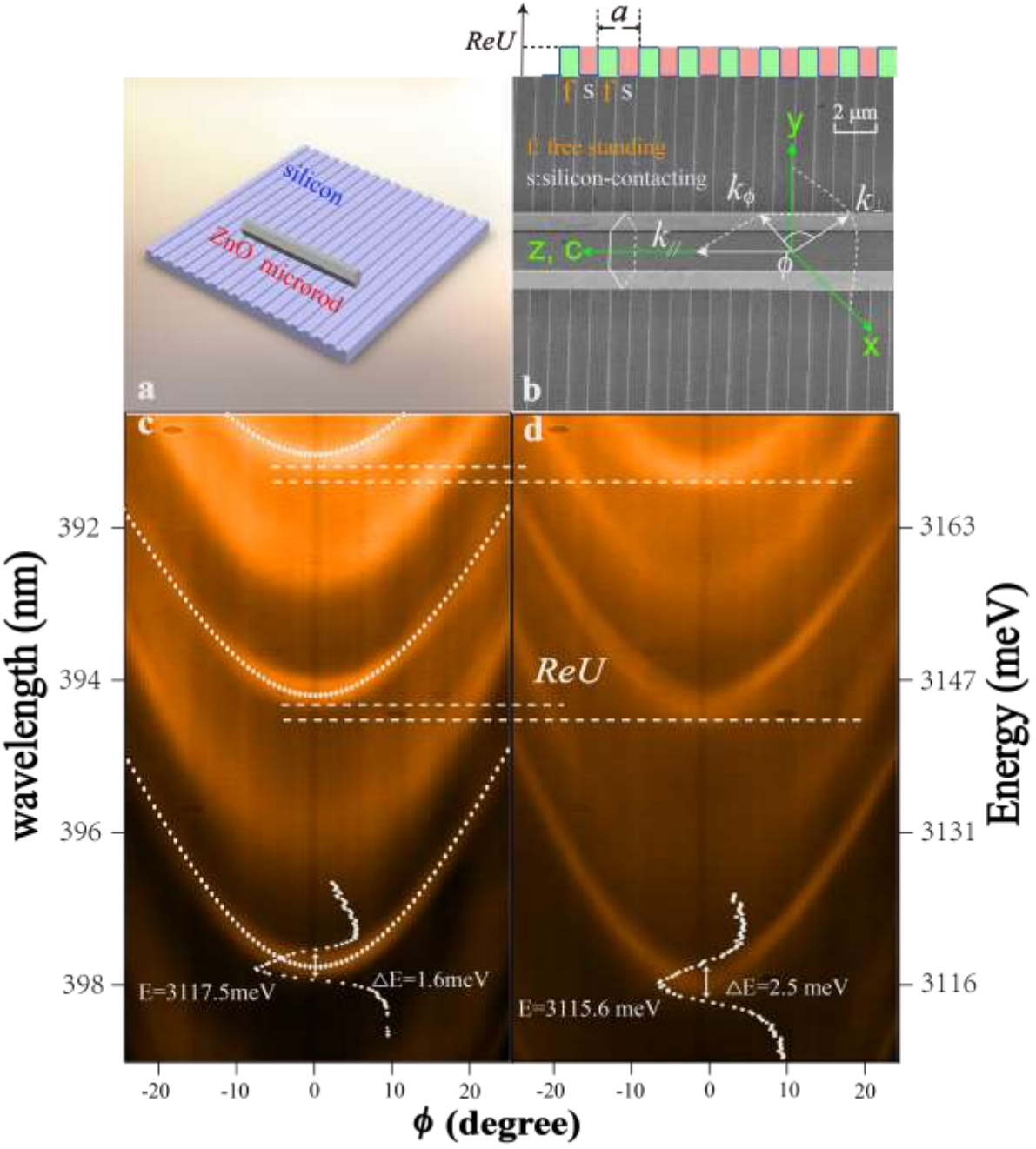
ReU
a
f s f s
2 μm
y
f: free standing
s:silicon-contacting
k_ϕ
$k_\perp$
$k_{//}$
z, c
ϕ
x
silicon
ZnO microrod
a
b
c
d
392
394
396
398
3163
3147
3131
3116
wavelength (nm)
Energy (meV)
ReU
E=3117.5meV
ΔE=1.6meV
E=3115.6 meV
ΔE=2.5 meV
-20
-10
0
10
20
-20
-10
0
10
20
ϕ (degree)

Figure 2

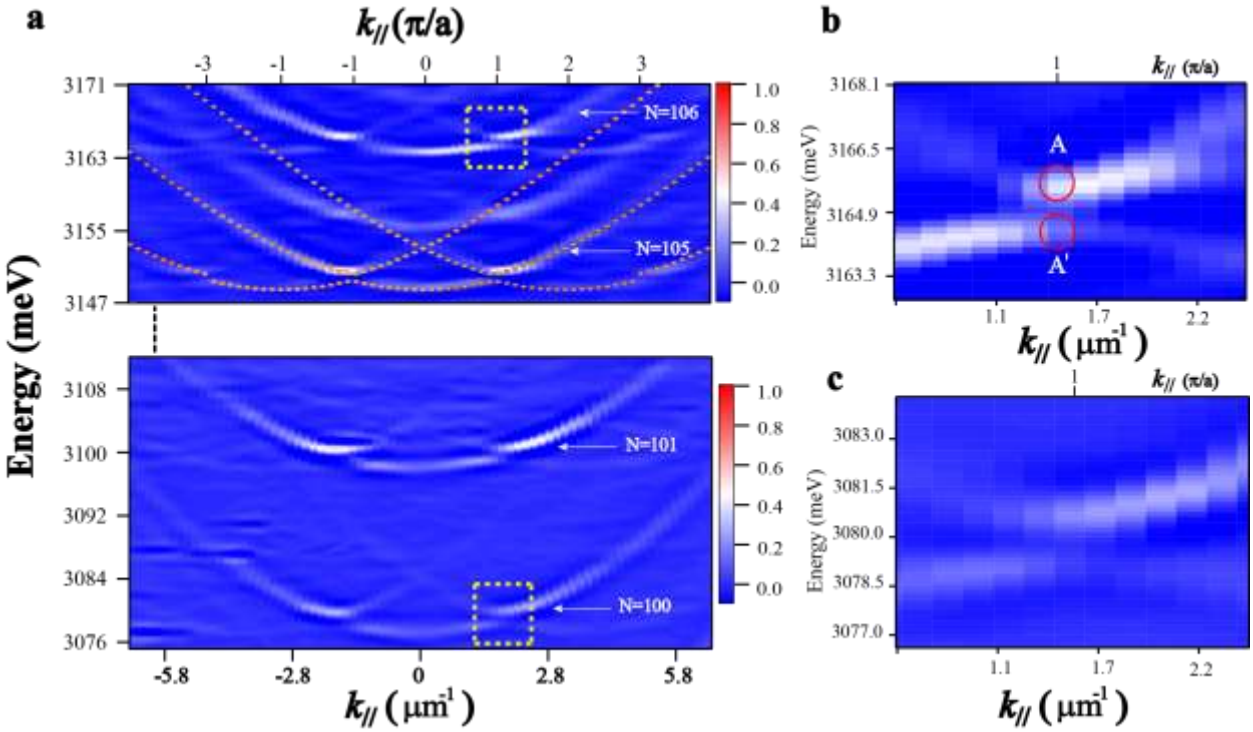

Figure 3

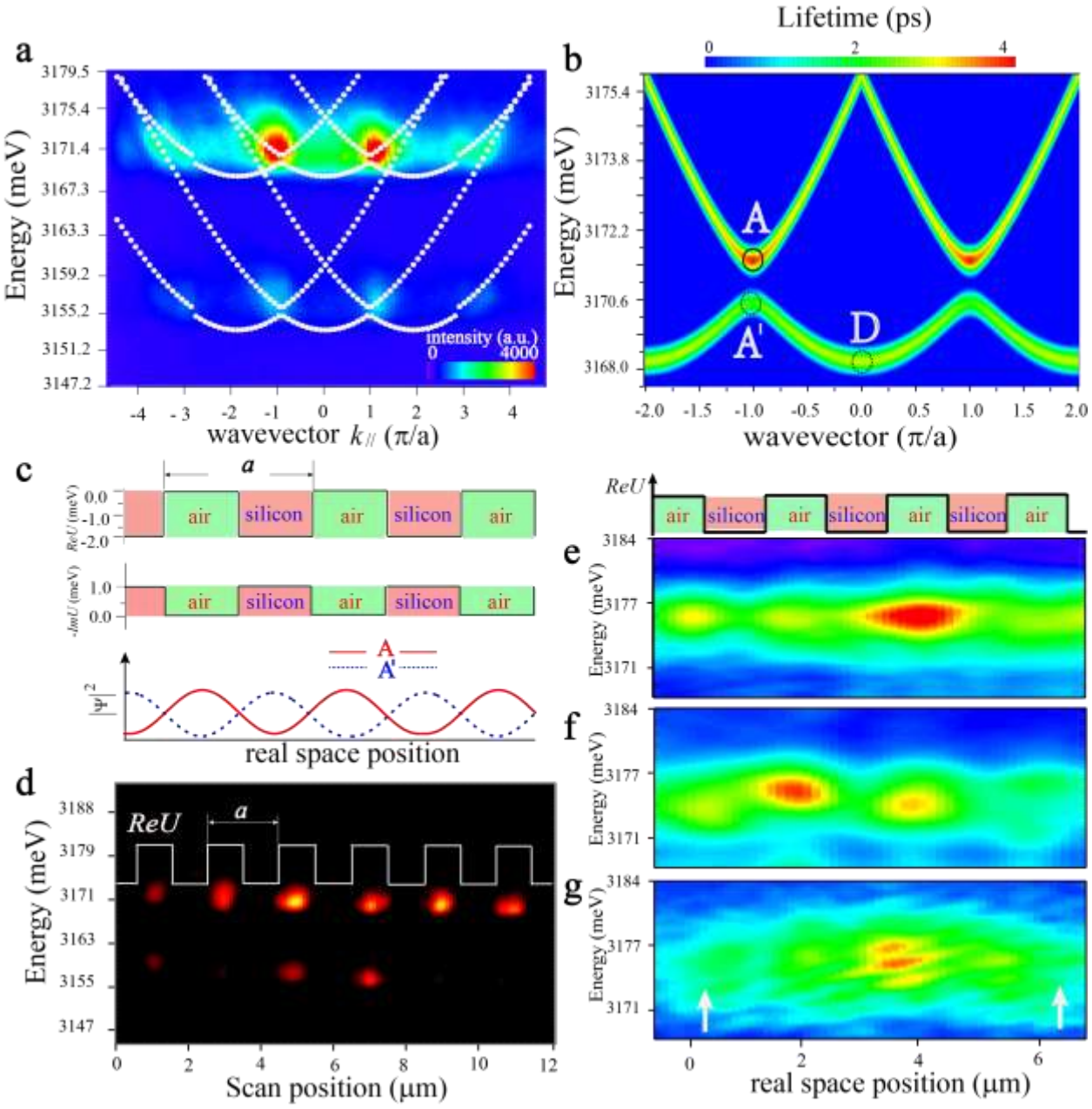
a
Energy (meV)
wavevector $k_{//}$ (π/a)
intensity (a.u.)
b
Lifetime (ps)
Energy (meV)
wavevector (π/a)
A
A'
D
c
a
air
silicon
ReU (meV)
-ImU (meV)
|Ψ|²
real space position
d
ReU
Energy (meV)
Scan position (μm)
e
f
g
real space position (μm)

Figure 4

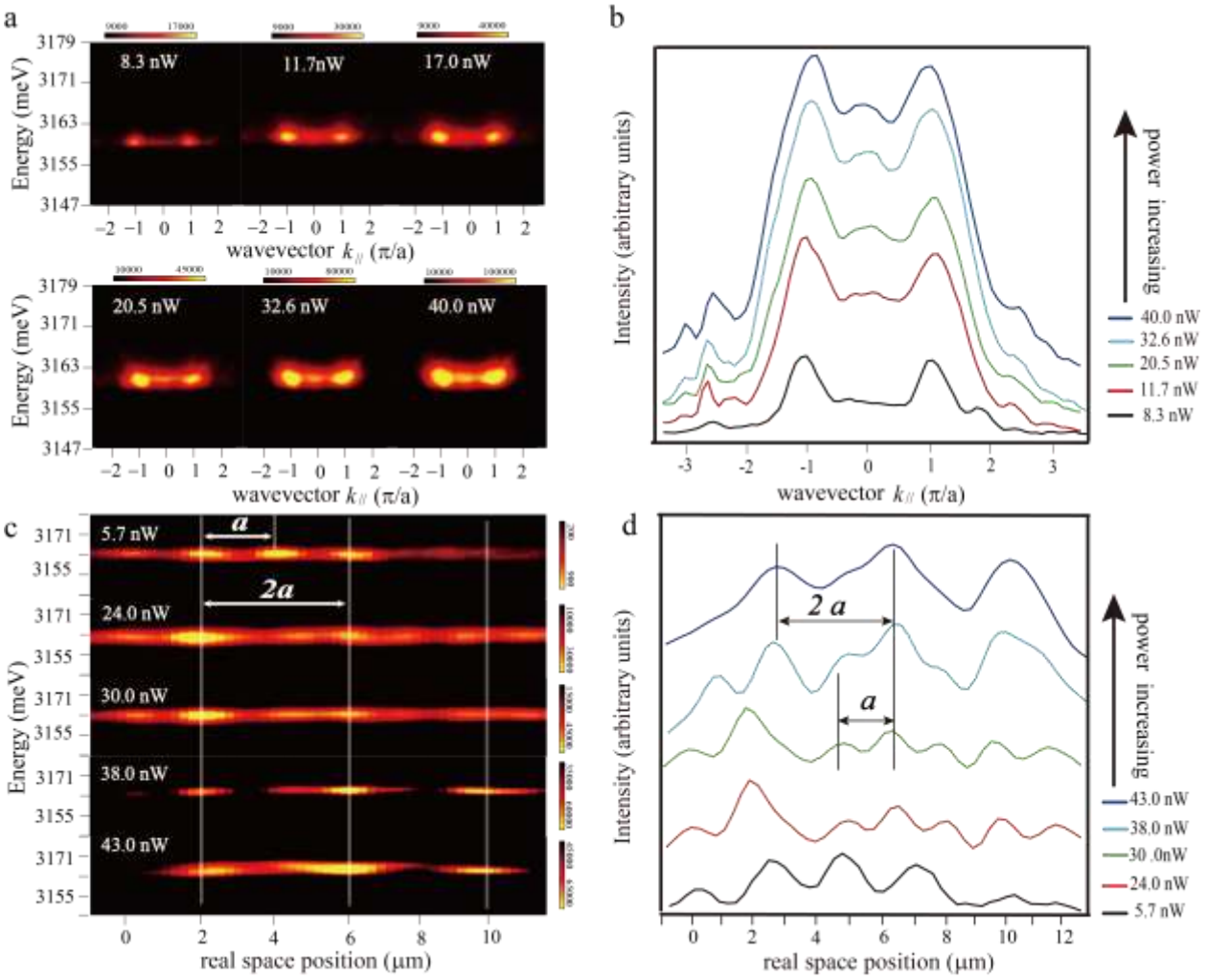
a
8.3 nW
11.7nW
17.0 nW
20.5 nW
32.6 nW
40.0 nW
Energy (meV)
wavevector $k_{//}$ (π/a)
b
Intensity (arbitrary units)
wavevector $k_{//}$ (π/a)
power increasing
40.0 nW
32.6 nW
20.5 nW
11.7 nW
8.3 nW
c
5.7 nW
24.0 nW
30.0 nW
38.0 nW
43.0 nW
a
2a
Energy (meV)
real space position (μm)
d
2 a
a
Intensity (arbitrary units)
real space position (μm)
power increasing
43.0 nW
38.0 nW
30 .0nW
24.0 nW
5.7 nW

Supporting Information

I. Calculation of the polariton lifetime

Below we present the details of the calculation of the polariton lifetime dependence on the Bloch wave vector. The polariton states with the energy $\hbar\omega$ are found from the simplest Kronig-Penney model

$$\left[-\frac{\hbar^2}{2m}\frac{\partial^2}{\partial z^2}+\hbar\omega_0-i\hbar\Gamma_0+U(z)\right]\Psi(z)=\hbar\omega\,\Psi(z) \tag{S1}$$

where the rectangular potential

$$U(z)=\sum_{n=-\infty}^{\infty}V(z-na),\qquad V(z)=\begin{cases}U_0, & |z|<a/2\\ 0, & |z|\geq a/2\end{cases} \tag{S2}$$

is induced for the polaritons by the grating in the silicon slice. Here, $\hbar\omega_0=3.169\,\text{eV}$ and $\hbar\Gamma_0=1.0$ meV are the polariton energy and radiative decay rate at the zero band wavevector along the microrod axis z for the unpatterned cavity; $m\sim0.5\times10^{-4}\,m_0$ is the polariton effective mass, m_0 is the free electron mass. Importantly, the potential (S2) is complex. The imaginary part of the potential describes the effect of the grating on the radiative decay rate of the polaritons. In our model we use $\text{Re}U_0=-2$ meV, $\text{Im}U_0=-1$ meV. The negative value of $\text{Im}U_0$ means that the decay rate is enhanced at the contacts of the microrod with silicon due to whispering gallery mode leakage to the high refractive index substrate. In the plane wave basis, the Bloch wave function with the wave vector $k_{\|}$ can be presented as $\Psi_{k_{\|}}(z)=e^{ik_{\|}z}\sum_{h=-\infty}^{\infty}\Psi_h\exp\left(2\pi ihz/a\right)$

and Eq. (S1) reduces to

$$\left[\frac{\hbar^2}{2m}(k_{\|}+2\pi h/a)^2+\hbar\omega_0-i\hbar\Gamma_0\right]\Psi_h+\sum_{h'=-\infty}^{\infty}U_{h-h'}\Psi_{h'}=\hbar\omega(k_{\|})\,\Psi_h, \tag{S3}$$

where

$$U_h=\begin{cases}U_0/2, & h=0,\\ U_0/(\pi h), & h=\pm1,\pm3,...\\ 0, & h=\pm2,\pm4,...\end{cases}$$

is the Fourier component of the potential (S2). The eigenstates of Eq. (S3) can be easily found analytically in the basis of nearly free polaritons. For the states at the band bottom (D) and at the lowest gap edges (A and A') the wave functions and energies read

$$D:\Psi_{k_{\|}=0}(z)=e^{ik_{\|}z},\quad \hbar\,\text{Re}\,\omega_D=\hbar\omega_0-\frac{\left|\text{Re}U_0\right|}{2},\quad \hbar\left|\text{Im}\,\omega_D\right|=\hbar\Gamma_0+\frac{\left|\text{Im}\,U_0\right|}{2},$$

$$A': \Psi_{k_\parallel=\pi/d}(z) = \cos(\pi z / a), \quad \hbar \operatorname{Re}\omega_{A'} = \hbar \operatorname{Re}\omega_D + \frac{\hbar^2\pi^2}{2ma^2} - \left|\operatorname{Re}U_0\right|/\pi\,,\ \hbar\left|\operatorname{Im}\omega_{A'}\right| = \hbar\Gamma_0 + \frac{\pi+2}{2\pi}\left|\operatorname{Im}U_0\right|,$$

$$A: \Psi_{k_\parallel=\pi/a}(z) = \sin(\pi z / a), \quad \hbar \operatorname{Re}\omega_A = \hbar \operatorname{Re}\omega_D + \frac{\hbar^2\pi^2}{2ma^2} + \left|\operatorname{Re}U_0\right|/\pi\,,\ \hbar\left|\operatorname{Im}\omega_A\right| = \hbar\Gamma_0 + \frac{\pi-2}{2\pi}\left|\operatorname{Im}U_0\right|.$$

The radiative decay rates are found as the imaginary parts of the eigen frequencies. In the case of very high quality factor of the free-standing microrod, $\hbar\Gamma_0 << \operatorname{Im}U_0$, the lifetime of the state A is about (π+2)/(π–2)~4.5 times longer than that of the state A' .

The dependence of the eigenmode lifetime on the Bloch wavevector and energy can be visualized by the PL spectrum,

$$I(\omega, k_\parallel) \sim \frac{1}{\pi} \operatorname{Im} \sum_n \frac{1}{\omega_n(k_\parallel) - \omega} \quad . \tag{S4}$$

Eq. (S4) is a rough approximation valid only in the linear-in-pumping regime. It can be obtained using the Langevin random sources approach, similarly to the case of quantum dots and quantum wells in the microcavity [1,2]. We also assume that the pumping rate is the same for all the modes *n*, the pumping is uncorrelated and wavevector independent, and neglect the relaxation processes. The spectral maxima of Eq. (S5) correspond to the polariton eigenmodes, the peak values are proportional to the eigenmode lifetime. In addition, for the case of high energy step-by-step excitation of the rod along the c direction (**Figure 3d**), the PL intensity for the given state (E, $k_\parallel$) can be described as follows,

$$I_{E,k_\parallel}(z) \sim |\Psi_{E,k_\parallel}(z)|^2\, \alpha_{E,k_\parallel}(z)\, \Gamma_0, \tag{S5}$$

where Ψ is the corresponding Bloch wavefunction, α is the generation rate of polaritons at the given state, and Γ_0 is the radiative decay rate. Under our experimental setup, PL signals are collected from the top surface of the microcavity. The signal intensity here is proportional to the normal radiative decay rate. Above the threshold, the generation rate α at the state A increases enormously because of the Bose stimulation.

II. Mixing of A and D states

Here we extend the theory of weak lasing and related mixing of two localized states [3] to the case of delocalized A and D states. The main difference with respect to Ref. [3] appears from the form of nonlinear terms that couple the states with distinct life times. We look for the wave function of the condensate as a superposition

$$\Psi(z) = C_{+1}\psi_A(z) + C_{-1}\psi_D(z), \tag{S6}$$

where $C_{+1} \equiv C_A$, $C_{-1} \equiv C_D$, $\psi_A(z) = \sqrt{2/L}\, u_A(z)\sin(\pi z/a)$ and $\psi_D(z) = \sqrt{1/L}\, u_D(z)$ are the wave functions of A and D states with $u_{A,D}(z+a) = u_{A,D}(z)$, and we have chosen $z = 0$ in the middle of a potential well. In general, these functions do not coincide precisely with those of the single-polariton *A* and *D* states, since one could have admixture of higher-lying *D* states, but they possess the same even-odd symmetry and can be chosen to be real functions. Spanning the Gross-Pitaevskii equation on the $\psi_{A,D}$ basis leads to the following equations for C_ξ ($\xi = \pm 1$, and we set $\hbar = 1$)

$$i\frac{dC_\xi}{dt} = \frac{i}{2}[W - \Gamma - \eta S + \xi(\gamma - i\varepsilon)]C_\xi + U_{\xi,\xi}\left|C_\xi\right|^2 C_\xi + U_{\xi,-\xi}\left(C_{-\xi}^2 C_\xi^* + 2\left|C_{-\xi}\right|^2 C_\xi\right). \tag{S7}$$

Here, W is the pumping rate of polaritons into the condensate, $\Gamma > \gamma > 0$ define the life-times of A and D states as $\tau_A = (\Gamma - \gamma)^{-1}$ and $\tau_D = (\Gamma + \gamma)^{-1}$, $\varepsilon = E_A - E_D > 0$ is the energy difference between A and D states. The nonlinearities in (S7) come from the term with $\eta > 0$ and $S = (|C_{+1}|^2 + |C_{-1}|^2)/2$, which accounts for the pumping saturation [4], and the polariton-polariton interaction terms, characterized by three interaction constants

$$U_{+1,+1} = U_0 \int \psi_A^4\, dx, \quad U_{-1,-1} = U_0 \int \psi_D^4\, dx, \quad U_{-1,+1} = U_{+1,-1} = U_0 \int \psi_A^2\, \psi_D^2\, dx. \tag{S8}$$

To find nontrivial solutions of (S7) it is convenient to introduce the 3D vector $\mathbf{S} = (C^\dagger \cdot \boldsymbol{\sigma} \cdot C)/2$, where we use the spinor $C = (C_{+1}, C_{-1})^{\mathrm{T}}$ and $\sigma_{x,y,z}$ are the Pauli matrices. For the components $S_{x,y,z}$ we obtain from (S7)

$$\dot{S}_x = -(\Gamma - W + \eta S)S_x - \varepsilon S_y - (\alpha_1 S + \alpha_2 S_z)S_y\,, \tag{S9a}$$

$$\dot{S}_y = -(\Gamma - W + \eta S)S_y + \varepsilon S_x + (\alpha_1 S + \alpha_2 S_z)S_x - \beta S_z S_x\,, \tag{S9b}$$

$$\dot{S}_z = -(\Gamma - W + \eta S)S_z + \gamma S + \beta S_x S_y\,, \tag{S9c}$$

and related equation for the total spin $\dot{S} = -g(S)S + \gamma S_z$, where

$$\alpha_1 = U_{+1,+1} - U_{-1,-1}\,, \quad \alpha_2 = U_{+1,+1} - 2U_{-1,+1} + U_{-1,-1}\,, \quad \beta = 4U_{-1,+1}\,. \tag{S10}$$

One stationary ($\dot{\mathbf{S}} = 0$) solution to the equations (S9a-c) describes the condensation into the pure A-state: $S_x = S_y = 0$, $S_z = S$, and $S = (W - \Gamma + \gamma)/\eta$. This solution appears at the threshold $W_1 = \Gamma - \gamma$. However, it can be shown that this condensate state becomes very quickly unstable with increasing W. Namely, the stability is lost at the second threshold

$$W_2 = \Gamma - \gamma + \frac{\eta\varepsilon}{(\beta - \alpha_1 - \alpha_2)}. \qquad (S11)$$

At this pumping the pure A-condensate continuously transforms into one of the two weak lasing states, which are characterized by increasing admixture of the D-state to the A-state for $W > W_2$. These weak lasing solutions to (S9a-c) are given by

$$S_z = \frac{g(S)}{\gamma}S, \qquad S_y = -\frac{g(S)}{f(S)}S_x, \qquad S_x = \pm\sqrt{\frac{(\gamma^2 - g^2)f(S)S}{\beta\gamma g(S)}}, \qquad \text{(S11a)}$$

$$g(S) = \Gamma - W + \eta S, \qquad f(S) = \varepsilon + \alpha_1 S + \alpha_2\frac{g(S)}{\gamma}S, \qquad \text{(S11b)}$$

where the average occupation S is found from $S^2 = S_x^2 + S_y^2 + S_z^2$ that gives

$$\beta S = \gamma\left[\frac{f(S)}{g(S)} + \frac{g(S)}{f(S)}\right]. \qquad \text{(S11c)}$$

The mixture of D and A states is defined by $S_z = \frac{1}{2}(|C_{+1}|^2 - |C_{-1}|^2)$. Since for $\varepsilon \gg \gamma$ one can neglect S_y compared to S_x, we conclude that the D state is formed either in-phase (the same sign) or out-of-phase (the opposite sign) with the A state. The ratio of the amplitude I_D of the peak at $k = 0$ to the amplitude I_A of one of the peaks at $k = \pm\frac{\pi}{a}$ is

$$R = \frac{I_D}{I_A} = 2\frac{|C_{-1}|^2}{|C_{+1}|^2} = 2\frac{[\gamma - g(S)]}{[\gamma + g(S)]}. \qquad \text{(S12)}$$

Analysis of equations (S11) shows that the function $g(S)$ decreases with increasing W, but saturates to value $g_{\min} = \gamma\alpha_1/(\beta - \alpha_2)$. Consequently, the ratio of the amplitudes of the peaks (S12) increases with increasing W and saturates to the value

$$R_{\max} = 2\frac{(\beta - \alpha_1 - \alpha_2)}{(\beta + \alpha_1 - \alpha_2)} = 2\frac{\left(3U_{+1,-1} - U_{+1,+1}\right)}{\left(3U_{+1,-1} - U_{-1,-1}\right)}. \qquad (S13)$$

From the wave functions $\psi_{A,D}(z)$ in the square-well periodic potential, that reproduces the experimental values of $\varepsilon = 2.2$ meV and the first gap of 0.7 meV, we can find $U_{+1,+1}/U_{-1,-1} = 1.43$ and $U_{+1,-1}/U_{-1,-1} = 0.90$, which results in $R_{\max} = 1.49$.

Supplementary references

1. Savona V, et al. (1996) Theory of polariton photoluminescence in arbitrary semiconductor microcavity structures, *Physical Review B* 53, 13051.

2. Averkiev NS, Glazov MM, Poddubnyi AN (2009) Collective Modes of Quantum Dot Ensembles in Microcavities, *JETP* 108, 836.

3. I. L. Aleiner, B. L. Altshuler, Y. G. Rubo, Radiative coupling and weak lasing of exciton-polariton condensates, *Phys. Rev. B* **85**, 121301 (2012).

4. J. Keeling, N. G. Berloff, Spontaneous rotating vortex lattices in a pumped decaying condensate, Phys. Rev. Lett. **100**, 250401 (2008).